Scale Invariance, Pattern Formation, and Disorder in Drying Colloids

V. N. Redmon IV

University of Illinois Urbana-Champaign
December 14, 2011

Abstract

Drying colloids have been shown to exhibit a rich variety of critical phenomena and pattern formations. They also have a wide range of practical applications. Here, a survey of the phenomena associated with drying colloidal suspension and a brief discussion of interesting applications is presented.

1 Introduction

Drying colloidal suspensions finds practical application in a wide variety of fields—from biology [5] to nano-structure formation [1]. These systems also display an array of interesting phenomena including a velocity dependent order to disorder transition on the microscopic level and a unique particle and interaction dependent macroscopic patterns. A seminal paper by Deegan *et al.* proposed a basic model for the fluid flow in a drying colloid. This basic model implemented the idea of contact line pinning, an unexplored idea at the time. They then tested the model by filming the movement of the particles through a microscope. The study of drying drops was extended in another paper by Deegan on pattern formation in the drops. More recently, Marín *et al.* used similar techniques to explore ordering of the deposited particles.

Aside from its fundamental interest and neat factor, pattern formation in drying colloids has a variety of applications. There are have been explorations for use in medical diagnostics, nano-structure creation, and agricultural seed analysis [4]. Further understanding the dynamics of microparticles in a drying solvents will only improve the quality and variety of practical applications of this phenomena.

In all studies presented, solutions are formed through mixing microspheres with water. Small drops, on the order of microliters, were dropped on to glass or mica slides. The drying dynamics were then imaged using a video camera attached to a microscope. The videos were then analyzed to explore the dynamics related to the study. In some cases fluorescent microsphere were used in imaging.

2 Coffee stains: rings from drying colloids

A commonly observed phenomena for many people in the world is that of the coffee stain. When a drip coffee of coffee falls from a cup and lands upon a surface, the liquid dries and leaves a ring shaped stain. This ring shaped stain results from the interplay between pinning the contact line—the line where the surface ceases to be wet—and evaporation of the solvent. Under circumstances for which the contact line is not pinned, i.e. pure DI water on a flat substrate, the radius of the drop expands to some maximum radius and then decreases as the liquid evaporates [2]. However, for pinned contact lines, liquid flows from inside to outside to replenish the evaporated liquid

and maintain the contact line. This results in the build up of particles at the contact line [3]. Figure 1 displays the mechanism for which the particles become deposited at the contact line. The evaporative flux exceeds the volume of the solvent near the contact line. Because the contact line cannot move, fluid and particles flow outward to replenish the liquid and maintain the contact line.
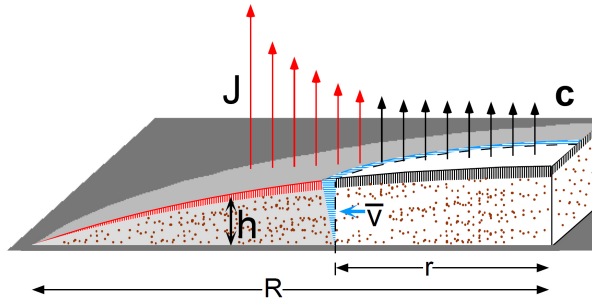

Figure 1: The mechanism for particle deposition at the contact line [3].

The evaporative flux is governed by mass conservation, $J(r) = -D\boldsymbol{\nabla}\phi$ where D is the diffusivity of the vapor and ϕ is the surface concentration of the vapor. After the drop is placed, the vapor concentration quickly establishes a steady state. The surface vapor concentration achieves some saturated concentration, ϕ_s and some background concentration ϕ_∞. The vapor profile follows the steady state diffusion equation, $\boldsymbol{\nabla}^2\phi = 0$. Solving for J yields, $J(r) \propto (R-r)^{-\lambda}$, where R is the drop radius, r is the radial position, $\lambda = \frac{\pi - 2\theta_c}{2\pi - 2\theta_c}$ and θ_c is the angle between the substrate and surface of the drop at the contact line. As the volume of the solvent decreases, the contact angle decreases to zero. This results in a diverging flux and subsequently a diverging fluid and particle velocity to maintain the contact line.

The model predicts power law growth of particle mass at the contact line, $M(R,t) \propto t^{2/(1+\lambda)}$. This prediction matches experiment well. Figure 2 presents a comparison of the model with experimental data. It shows that during the beginning of the deposition, the contact line mass increase with the predicted power law. The data presented covers approximately 10-250 sec. The overall drying time for these samples were 800 sec. The inset shows a similar power law dependence for a drop with a 1300-sec drying time.

In further study Deegan presented an exploration of the conditions for which patterns form in a similar system [2]. The notable difference between
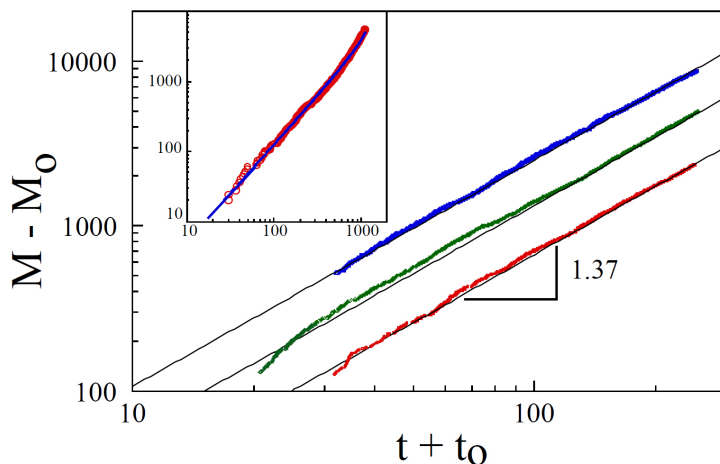
Figure 2: The power law dependence of the mass of the contact line [3]

this experiment and the initial experiments was the substrate. A desire in this experiment was to prepare a nearly perfectly flat substrate such that presence of the solute was the only contributor to pinning. This was realized through use of cleaved mica. An experiment using drops of filtered DI water—no microspheres—showed the surface to be, to a high degree, atomistically flat. A density of 1 pinning site per cm^2 was found.

The lack of pinning points is crucial for pattern formation. This requirement allows the contact line to be defined by the energetics of the drying colloid. Pinning at the contact line has some energy barrier for depinning. This energy barrier would be tremendous if the substrate provided many pinning sites—as evidenced by a lack of unique forms in Ref [3].

3   Depinning scale invariance

Depinning of the contact line occurs at late times in the drying. The drop expands to its maximal radius as it evaporates the contact line remains pinned until very little solvent remains. At this point the contact line may depin, retract, and take a trail of particles with it. One of the first tests conducted was an analysis to depinning time verse solid volume fraction. This resulted in a power law dependence of the normalized depinning time against the solid volume fraction , t/t_f where t_f7 is x-intercept of the linear portion of the evaporation curve **IMAGE???**. Figure **??** shows this dependence. The

4

log-log plot yielded power law exponent of 0.26 ± 0.08. The author also conducted this experiment for situations with a far slower drying time. The normalized depinning time for slow evaporation was found match the normalized time for faster evaporation, suggesting that depinning results from self organization of the particles. The second study explored the dependence
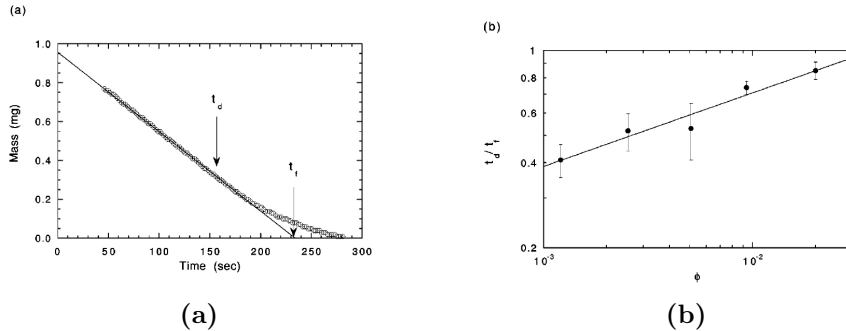

Figure 3: (a) The extrapolated, effective drying time. [2] (b) The normalized depinning time plotted—log-log—against solid fraction. The graph reveals a power law dependence on solid fraction [2]

of the narrowest width of the contact line on solid volume fraction. This exploration too yielded a power law dependence. Inconsistencies drop volume required that width of the contact line be normalized by the drop radius. This experiment was conducted for 1-μm and 0.1-μm microspheres. Figure 4 presents a log-log plot of depinning width vs solid volume fraction for both particles. The 1-μm particles yielded an exponent of 0.86 ± 0.10 and the 0.1-μm particles yielded an exponent of 0.78 ± 0.10.

The scale invariance of these two results indicate that depinning is a self organized phenomena.

4 Pattern formation

Depinning events also cause patterns to form. After long evaporation times, the forces that contribute to depinning and pinning the contact line have similar magnitudes. As depinning events and the contact line recedes material is taken from the ring and deposited within the ring. Figure 5 shows, for different volume fractions, the patterns that form after the contact line recedes. Qualitatively, the different concentrations follow a similar pattern consisting of concentric circles. It is interesting to note that distinct concentric circles form in (a) and (d) of Figure 5 while (c) and (d) have larger,
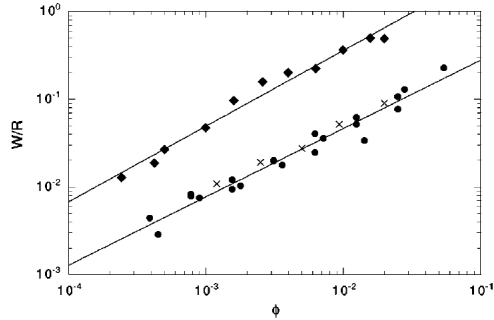
Figure 4: A log-log plot of the normalized-contact-line width vs. solid fraction. This graph reveals a power law dependence on the volume fraction. The circles correspond to 1-μm spheres and the squares correspond to 0.1-μm spheres. In reality the data overlaps. The data for the squares were scaled to separate the lines [2]

more spread out concentric rings. Zooming in on the images reveals further patterns.
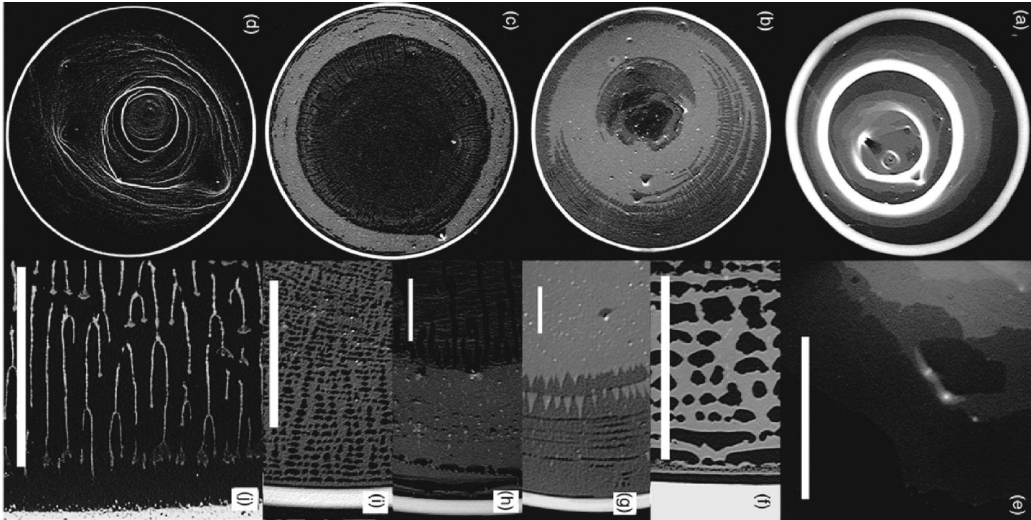
Figure 5: Images and close-ups (directly below overall image) of patterns formed for different initial concentrations from 0.1-μm particles: (a)-1%, (b)-0.25%, (c)-0.13%, (d)-0.063%. The images directly below the large images are close-ups of the patterns formed for the corresponding concentrations [2]. For printing purposes, the image was rotated.

Images of the patterns for different concentrations using the 1-μm spheres revealed a trend that similar to the 0.1-μm case—the pattern remained qualitatively similar over a significant volume fraction range.

Another interesting experiment conducted by Deegan explored patterns formed when a surfactant was introduced. New and interesting patterns formed as a result of a changing interaction strength mediated by the ionic surfactant. In this case, the volume fraction remained the same, and the surfactant concentration varied. Qualitative results of the experiment are shown in Fig. 6.
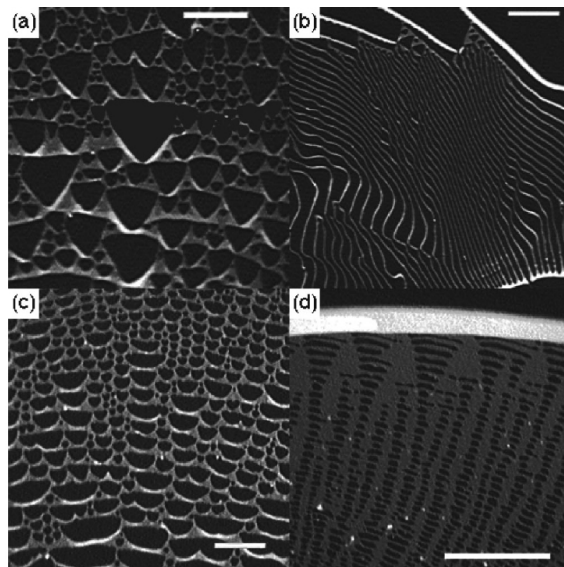

Figure 6: Patterns formed from [2]

The work of presented in Ref. [2] experimentally reveals several characteristics of the drying colloid that indicate self organization and critical phenomena similar to that of many other pattern forming systems. A review of literature reveals no evidence of phenomenological theories regarding this system. However, it seems that, in principle all of the pattern formation techniques could be applied. Several challenges involve with modeling these systems arise from the geometry and challenges associated with calculating the free energy. Deegan suggests that a well-reasoned experiment that simplifies the geometry could jumpstart further theoretical explorations of these systems.

5 The order-disorder transition in drying colloids

Another example of interesting phenomena in colloidal suspensions is seen in the work of Marín *et al.* [?]. In this work an order to disorder transition was observed. The authors place a 3μL droplet of colloidal particles (0.5μm-2μm fluorescent polystyrene particles) onto a glass microscope slide and image the drop, via fluorescent light, from below. They also image the drop from the side using a long distance microscope and a CCD camera.

The experiment proceeded through imaging the particles in the colloidal drop as the solvent evaporated. Upon evaporation, the ring stain was observed. Looking closer at the particles in the stain revealed a radial dependent disorder to order transition. In the ordered state there were two different lattice structures—square and hexagonal. The structure of the ring can be seen in Fig. 7.
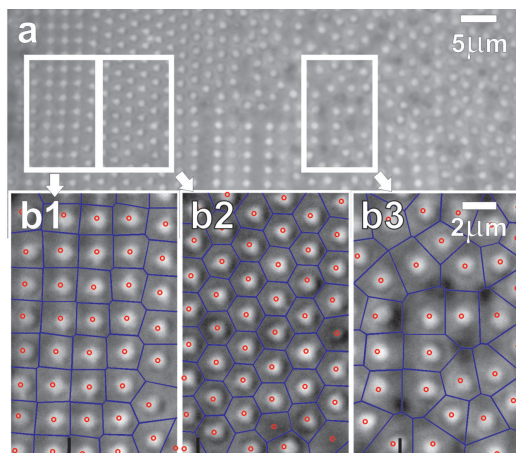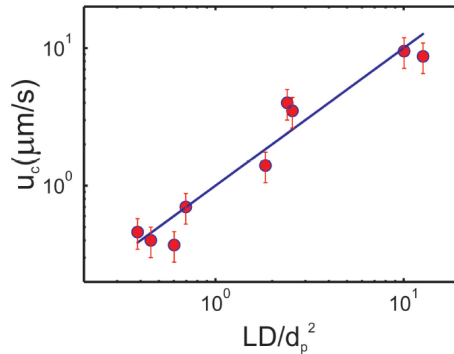

Figure 7: Different structures for particles deposited from a drying colloid.

An analysis of the images leading up to the evaporated state revealed that the velocity of outward flowing particles increased rapidly as the solvent finished evaporating. It was found that particles arriving at the ring before this rapid increase organized into an ordered stated. However, particles arriving after this increase in speed remained in the disordered state. To exhibit the effect of "rush hour" on the structure the authors compared the velocity of the particles to the structure in the video. Plotting outward particle the velocity as a function of time shows the "rush hour." Comparing the

outward velocity with the evaporation time at which ordering occurs yields some critical velocity, u_c, for the order-disorder transition. The model developed in the paper matches the data quite well. From this model, the authors were able to accurately predict the critical velocity. Through comparing the times scale for the diffusivity time scale with the the hydrodynamic time scale yields a critical velocity, $u_c \propto D/(n_p^{-1/3}d_p^2)$. Here, D is the diffusivity, n_p is the particle concentration, and d_p is the particle diameter. A plot of the predicted critical velocity against the measured velocity is shown in Fig. 8

Figure 8: Different structures for particles deposited from a drying colloid.

The results of this study suggest a novel method to prepare organized colloidal crystals. By maintaining a low particle velocity the width ring can be made large and the order of crystal engineered.

6   Applications of drying colloids

The critical phenomena and self organization associated with drying colloid have found potential applications in several areas. Two unique applications that are currently being explored are the use of self organization in drying drops of biological fluids as a method for disease diagnostic (Ref. [5]) and patterns formed by evaporating wheat grain leakages as a tool for seed quality testing (Ref. [4]). In both of these systems, the interaction between the suspended particles cause unique patterns. The interactions change depending on different particles and result in different patterns. These different

patterns can then be correlated with the variety of disease or quality of seed. In the case of the seed analysis, the patterns formed were fractal like and the different seed leakages corresponded to different fractal dimensions. For the medical diagnosis, several different fluids of patients with different diseases were tested. After the samples dried there was noticeable differences in the deposited structure. Additionally, the physical properties of the drying drops were explored using acoustic-mechanical impedance measurements.

7 Conclusion

The study of drying colloids presents many different and interesting research lines. These systems exhibit potential for continued study of fundamental pattern forming and critical phenomena. They also present many variety of potential applications. Research into these applications could provide new technologies in a variety of areas including, but not limited to, medical diagnostics, agricultural diagnostics, and nano-structure construction. Both fundamental study and research into practical applications are important for furthering the field.

References

[1] Terry P. Bigioni, Xiao-Min Lin, Toan T. Nguyen, Eric I. Corwin, Thomas A. Witten, and Heinrich M. Jaeger. Kinetically driven self assembly of highly ordered nanoparticle monolayers. *Nat Mater*, 5(4):265–270, April 2006.

[2] Robert D. Deegan. Pattern formation in drying drops. *Phys. Rev. E*, 61:475–485, Jan 2000.

[3] Robert D. Deegan, Olgica Bakajin, Todd F. Dupont, Greb Huber, Sidney R. Nagel, and Thomas A. Witten. Capillary flow as the cause of ring stains from dried liquid drops. *Nature*, 389(6653):827–829, October 1997.

[4] Maria Olga Kokornaczyk, Giovanni Dinelli, Ilaria Marotti, Stefano Benedettelli, Daniele Nani, and Lucietta Betti. Self-organized crystallization patterns from evaporating droplets of common wheat grain leakages as a potential tool for quality analysis, 2011.

[5] T.A. Yakhno, V.G. Yakhno, A.G. Sanin, O.A. Sanina, A.S. Pelyushenko, N.A. Egorova, I.G. Terentiev, S.V. Smetanina, O.V. Korochkina, and E.V. Yashukova. The informative-capacity phenomenon of drying drops. *Engineering in Medicine and Biology Magazine, IEEE*, 24(2):96 –104, march-april 2005.